Bulg. J. Phys. **43** (2016) 54–63

Self-Catalytic Growth of InN Nanowires

P.T. Terziyska[1], **K.S.A. Butcher**[2,3]

[1]Institute of Solid State Physics, Bulgarian Academy of Sciences, 72 Tzarigradsko Chaussee Blvd., 1784 Sofia, Bulgaria

[2]Semiconductor Research Laboratory, Department of Electrical Engineering, Lakehead University, 955 Oliver Rd, Thunder Bay, ON P7B 5E1, Canada

[3]MEAglow Ltd. Box 398 2400 Nipigon Rd., Thunder Bay, ON P7C 4W1, Canada

Received *20 February 2016*

Abstract. In this paper we review our results on self-catalytic growth of InN nanowires, grown from In metal rich conditions by the Migration Enhanced Afterglow (MEAglow) technique. We present a short overview of the different growth methods that have been applied to produce InN nanowires and we discuss the self-catalytic growth mechanism for InN nanowires. We then present our experimental results on the self-catalytic and selective area growth of InN nanowires that show evidence for the nucleation and the growth mechanism of the InN nanowires under In metal rich conditions. Selective area growth on sapphire substrates is also discussed.

PACS codes: 81.07.Gf, 81.16.Hc

1 Introduction

InN is currently receiving much attention from a technological and fundamental point of view. Due to its direct band gap, superior transport properties (low electron effective mass, high saturation and drift velocity) and its ability to form ternary and quaternary alloys, InN has considerable potential for application in optoelectronic devices in a broad spectrum ranging from the near IR to the UV. The formation of a surface accumulation layer on some orientations of InN eases the fabrication of low resistivity ohmic contacts. The high electron mobility of the InN makes the conductivity of nanowires particularly sensitive to surface charge modulation which can be very useful for applications in chemical and bio-sensors.

A number of different growth methods have been applied to produce InN nanowires and nanorods, namely solid-liquid-solid [1], chemical vapour deposition[2-11], vapour phase epitaxy [12-15] and molecular beam epitaxy [16,17]. The substrates most commonly used for InN nanowire growth are Si and sapphire [14]. Self-catalytic [2,10,11,18] as well as Au metal catalyst [1,3,4,19]

growth of InN nanowires has also been reported. To minimise impurity contamination it is desirable to produce catalyst free (or self-catalytic) nanostructures. In this work we will first briefly describe the self-catalytic 1D growth of InN nanowires by the MEAglow technique which is a type of plasma assisted chemical vapour deposition technique, then we will present our experimental results of InN nanowires grown by the MEAglow technique using indium rich conditions [20,21].

2 Self-Catalytic Growth of InN Nanowires by the MEAglow Technique

2.1 Overview of the MEAglow technique

Growth of epitaxial layers. MEAglow is a low temperature migration enhanced chemical vapour deposition (CVD) technique for the growth of group III-nitrides and other compound semiconductors. For this film growth technique pulsed deposition is used to improve the crystal quality of materials grown at relatively low temperatures. During growth metalorganic pulses form one or more metal adatom layers on the substrate surface. The limitation of low adatom mobility at lower temperatures is therefore overcome by dosing the whole crystal surface with metal. The metal layer is then subsequently nitrided with active nitrogen species from a plasma source [22-24]. The metal deposition and subsequent nitridation can be done in multiple cycles to achieve thick nitride layers. The active nitrogen species are supplied from a nitrogen gas plasma, created in a hollow cathode. This plasma source has the advantage of having a high electron density (similar to inductively coupled plasma sources) but without the accompanying oxygen contamination issues [23]. The method allows epitaxial growth of high quality nitride layers [24].

Growth of nanowires. For very metal-rich conditions metal droplet formation occurs, which was shown in our previous work [20] to be favourable for the metal-rich growth of catalyst-free InN nanowires. The use of active nitrogen plasma species allows a higher penetration depth in the In-metal droplets and a higher diffusion rate of the nitrogen through the droplet to the interface In/InN where the growth occurs.

2.2 Self-Catalytic growth of InN nanowires from In-rich conditions by MEAglow

A detailed and profound study of the self-catalytic growth mechanism of single crystal III-V and II-VI binary, ternary and quaternary nanowires and whiskers by chemical vapour deposition has been provided by S.N. Mohammad in Ref. [25]. The formation of liquid droplets and seeds, and the nucleation and the creation of nanowires, have been discussed in detail in his work.

Self-catalytic growth can be divided into the following stages – (1) creation and retention of liquid In-metal droplet, (2) adsorption and incorporation of nitrogen species from the ambient atmosphere in the liquid droplet, (3) nucleation and axial growth of the nanowire.

Formation of droplets. The formation of metal droplets on the substrate surface occurs on the small grains of the InN nuclei initially formed on the substrate surface, or on sharp needles on the substrate itself. The molten metal accumulates in the form of droplets around these sharp edges or grains.

Adsorption and incorporation of species in the metal droplet. Active nitrogen plasma species and InN molecules formed in the chamber ambient are incorporated in the In metal droplet and condense on the liquid-solid interface. A supersaturation of the droplet is required for the further 1D nanowire growth.

Nucleation and axial growth. At the liquid-solid interface formed by the droplet and the seed, occurs a break of the symmetry of the isotropic crystal, which is crucial for the initiation of one-dimensional (1D) nanowire growth [25]. Thus each liquid droplet tends to induce and dictate the nanowire growth. The nucleation at the liquid solid interface is the most energetically favoured process so it supresses any other nucleation in the volume of the droplet. The growth of the nanowire occurs at the liquid-solid interface. As the supersaturation continues and the liquid droplet remains liquid, the 1D nanowire growth takes place.

The as described growth mechanism is self-catalysed, because the liquid metal droplet is the catalyst and at the same time is one of the constituent elements of the nanowire. It is a metal liquid without the need of foreign element catalysts (such as Au, Ag, etc.) which can introduce undesired contamination.

3 Experimental Results for Self-Catalytic Growth of InN Nanowires by MEAglow Technique

In this section we will first present our initial results on InN nanowires grown on c-plane sapphire, which are randomly oriented. Then we will present our experimental results on vertically oriented nanowires grown on selected areas of the sapphire substrate. Finally we will show experimental proof that the growth process is similar to the process of liquid phase epitaxy and occurs at the liquid-solid interface between the In-metal droplet and the body of the nanowire from the supersaturated indium melt.

A standard procedure used for the growth of our InN nanowires is described as follows. Prior to the film growth the substrate (one-side polished c-plane sapphire) was heated in air to 1050°C to eliminate polishing damage. The sapphire was then loaded in the MEAglow system, heated for one hour under nitrogen gas flow at a temperature of 490°C and was then subsequently nitrided for 1 minute

with the nitrogen plasma. A nitrogen flow rate of 1000 sccm, a radio frequency (RF) power of 100 W and a gas pressure of 750 mTorr were used for the nitridation procedure. The substrate temperature during the growth was maintained at 490°C. Try-methyl indium (TMI), used as the indium source, was delivered as pulses of 10 seconds with 0.6 sccm of TMI flow. The plasma was on continuously during one cycle at a nitrogen flow rate of 500 sccm and RF power of 300 W. The total duration of one cycle was 30 seconds and the number of cycles was 1000. The pressure in the growth chamber was 1310 mTorr.

The morphologies of the resulting products were characterized using a SU-70 analytical ultra-high resolution Schottky Emission scanning electron microscope (SE-SEM). The structural properties were characterized by XRD measurements and Raman scattering. XRD measurements were performed using a PANalytical X'Pert Pro MRD diffractometer with a copper anode. The Raman spectra were measured in backscattering geometry in the range 300–700 cm^{-1} on a HORIBA Jobin Yvon Labram HR visible spectrometer equipped with a Peltier-cooled CCD detector. The 633 nm line of a He-Ne laser was used for excitation. The spectral width was 1.5 cm^{-1}, and the absolute accuracy 0.5 cm^{-1}.

3.1 Nucleation and 1D growth of the InN nanowires

An SEM micrograph of the as grown randomly oriented products is shown in Figure 1. The nanowires are approximately 2 μm long and 100–200 nm in diameter, containing a spherical In-metal droplet on top.

The different stages of nanowire growth, from the droplet formation and nucleation to the start of the growth for the nanowires, are shown on the SEM

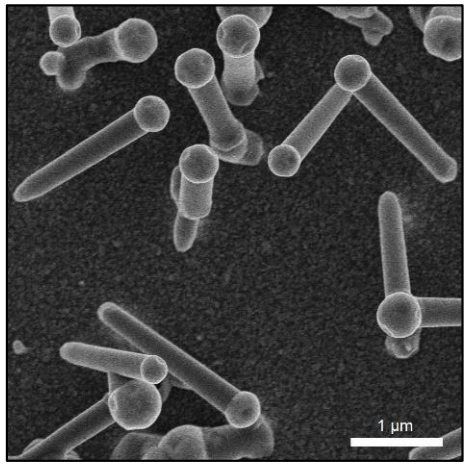

Figure 1. SEM micrographs of the as-grown sample for 1000 cycles.

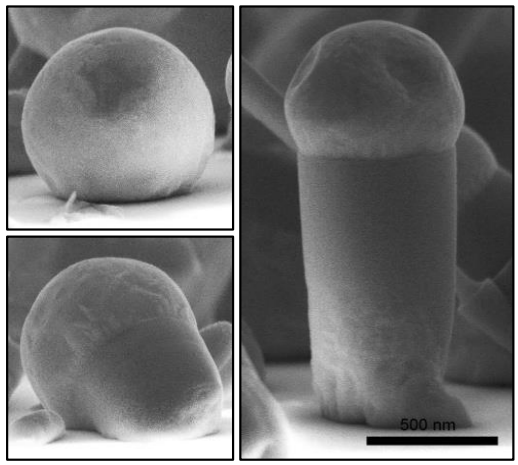

Figure 2. SEM micrographs of different stages of the InN nanowire growth: from droplet to the formation of the nanowire.

micrographs of Figure 2. The growth direction and the shape of the nanowire body are determined by the liquid In-metal droplet. The growth mechanism is basically a form of liquid-phase-epitaxy. The crystal growth occurs at the solid-liquid interface from the supersaturated In-metal droplet. The nanowire diameter is consequently determined by the size of the droplet and its shape is determined by the droplet shape.

InN nanowires grown from nitrogen rich conditions have cross-section determined by the crystal habit (cubic or hexagonal) in contrast to the nanowires shown here, whose shape is determined by the shape of the indium droplet.

3.2 Vertically oriented nanowires

We will now focus on the nucleation and the growth in vertical direction of self-catalytic InN nanorods grown under indium rich conditions on sapphire substrates by the MEAglow technique. These results were presented in Ref. [21].

Vertically oriented nanowires were grown on selective areas of sapphire substrates exhibiting sharp needles of approximately 9 nm in height. This unintentional patterning of some commercial sapphire substrates was observed after the annealing and subsequent plasma nitridation. A large area SEM micrograph (Figure 3(a)) and an 8×8 μm AFM topography image (Figure 3(b)) of the sapphire substrate after the nitridation step show the presence of two different surface areas – relatively rough triangular areas (RMS = 0.6 nm) surrounded by a flat (RMS = 0.1 nm) area. The AFM topography image shows that the rough areas are covered by small ~ 9 nm high sharp AlN based needles. Similar AlN needles have been reported to appear on sapphire substrates after nitridation as

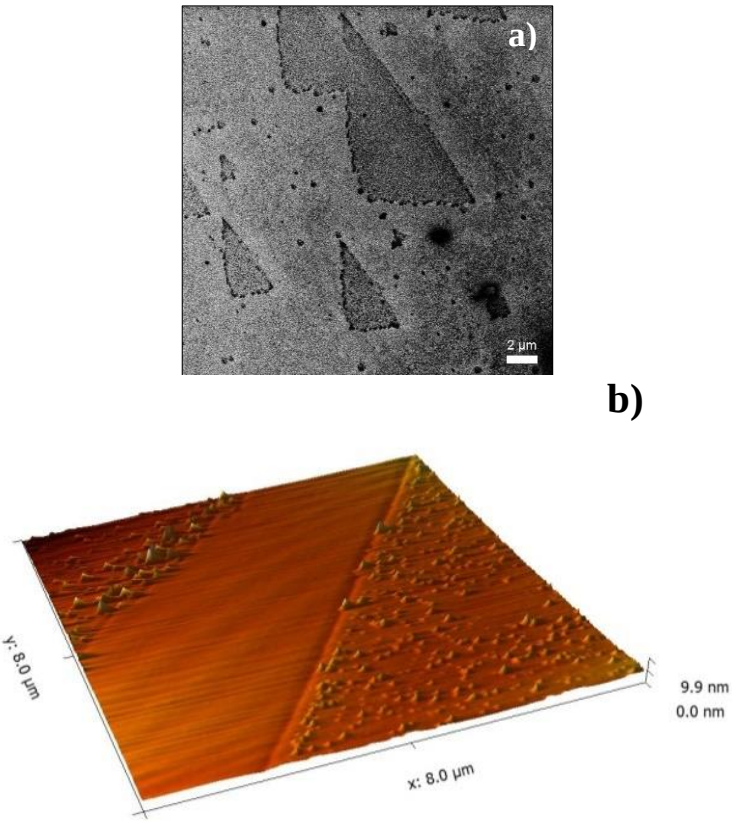

Figure 3. Sapphire substrate after annealing and nitridation: (a) SEM bird's-eye-view micrograph: triangular areas of different contrast can be distinguished; (b) AFM topography image on a surface including parts of both rough triangular (RMS = 0.6 nm) and the surrounding flat (RMS = 0.1 nm) areas.

a result of stress accommodation in the AlN layer formed on the surface of the sapphire during nitridation [26]. Needles could therefore be obtained by over-nitridation of unmasked areas of the sapphire substrate. In this case the process would be selective.

The as-grown nanorods on these unintentionally patterned c-sapphire substrates are presented in Figure 4. As can be seen from the large area SEM micrographs (Figure 4(a)), the triangular areas observed on the substrate (Figure 3) are replicated after the InN growth. Nanorods perpendicular to the substrate surface are grown on these areas (Figures 4(b,c)). Indium droplet formation takes place preferably on the sharp apices of the sapphire needles in these particular areas. Tiny spherical droplets form on the tips and attract nitrogen and indium reactant atoms or InN molecules with higher rate than droplets with smaller curvature.

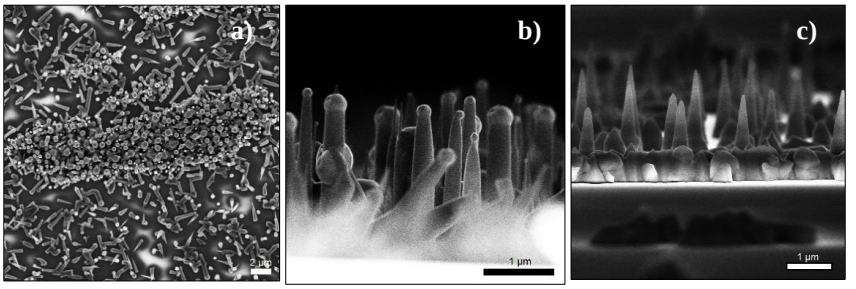

Figure 4. SEM micrographs of the as grown InN nanorods: (a) bird's-eye-view and (b) side view of the InN nanorods without indium desorption step at the end; (c) side view of the InN nanorods with 5 min indium desorption step at the end of the growth process.

This means that the nucleation of InN takes place with highest probability on the sharp tips (on the areas of triangular shape (Figure 3)). The In droplets undergo supersaturation leading to nucleation of InN underneath, on the top of the sapphire peak apex. Following the nucleation, straight nanorods perpendicular to the substrate start to form on these areas (Figures 4(a,b)) [25,28-31]. Additionally, on the rougher areas of the substrate, the three dimensional growth has increased support of the nanorod at their base. Contrarily, the InN nanorods are very weakly attached to the substrate surface in the smooth areas (Figure 3) so that they cannot remain straight (Figure 4(a)). This way, the needles serve as a support of the nanorods, better anchoring them to the substrate and favouring the growth in a vertical direction.

Two different samples are presented for comparison – with (Figures 4(a, b)) and without (Figure 4(c)) indium metal droplet on their tops. For the second sample the growth temperature is 500°C and an additional metal desorption step at the end of all cycles was introduced, during which the pressure in the growth chamber was set to zero for 5 min keeping all the other parameters unchanged. The as obtained nanorods have conical tips. This morphology provides evidence that the growth continues from the supersaturated indium melt. This solution remains super saturated due to the continuous desorption of the In-metal solvent. The epitaxial growth continues until all the In-metal solvent is consumed for the formation of InN and/or desorbed. In the case without indium desorption at the end (Figures 4(a,b)), the growth continues until the indium metal droplet remains supersaturated. In this case the diameter of the nanorod remains unchanged as it is determined by the In droplet diameter which does not change at the end compared to the sample in Figure 4(c). The diameter of the nanorods is smaller in comparison with the second sample due to the elevated temperature of the growth (510°C instead of 500°C). The indium metal droplet remains on the apex of the nanorods.

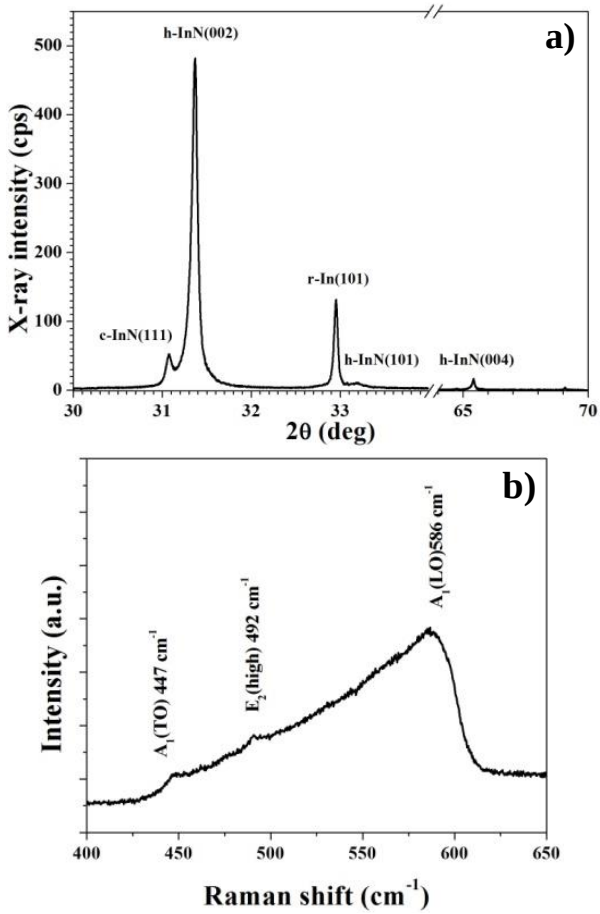

Figure 5. Typical (a) XRD and (b) Raman spectra of the InN nanowires (containing In-metal droplets on top).

The XRD spectrum of a typical product with In-metal droplets on top is shown in Figure 5. Two different phases of InN – hexagonal (h-InN) and cubic (c-InN) and one rhombohedral phase of In-metal (r-In) can be indexed. The c-InN(111) peak is at 31.06° 2θ and has a FWHM = 0.07° 2θ (252 arcs) and the h-InN(002) peak is at 31.35° 2θ and has a FWHM = 0.06° 2θ (216 arcs). These small FWHM values indicate that the nanowires have very good crystal structure and are relatively stress free. The preferred orientation and the growth direction are (001) (the (002) plane is parallel to the substrate surface). The presence of cubic InN or of mixtures of hexagonal and cubic phases has also been reported in Ref. [3,4,6].

Figure 5(b) shows a typical Raman spectrum for the nanowires. The Raman spectrum of the vertically oriented nanorods shows the presence of the hexagonal InN A_1(TO), E_2(high) and A_1(LO) at 447, 492, and 586 cm^{-1} respectively [3,27].

4 Conclusion

In summary, we have demonstrated the self-catalytic growth of InN nanowires on (0001) sapphire, under In-rich conditions, using the Migration Enhanced Afterglow (MEAglow) growth technique. The growth of the nanowires is a kind of liquid phase epitaxy from the supersaturated In melt in the droplet and occurs at the solid liquid interface between the In-metal droplet and the InN body of the nanowire. The formation of droplets forms preferentially on sharp apices on the substrate. In case of the growth on the sharp needles, the nanowires are very well anchored to the substrate and aligned in a direction perpendicular to the substrate, along the sharp needles. Selective area growth was also discussed. In the case of sapphire substrates, sharp needles can form on (selected) areas that are exposed for longer time under nitrogen plasma. The growth of vertically oriented InN nanowires will be selective on such substrates.

Acknowledgements

The author would like to acknowledge the project INERA REGPOT-2012-2013-1 NMP: Research and Innovation Capacity Strengthening of ISSP-BAS in Multifunctional Nanostructures.

References

[1] Z.H. Lan, W.M. Wang, C.L. Sun, S.C. Shi, C.W. Hsu, T.T. Chen, K.H. Chen, C.C. Chen, Y.F. Chen, L.C. Chen (2004) *J. Cryst. Growth* **269** 87-94.

[2] S.-H. Yun, S. Kissinger, D.W. Kim, J.-H. Cha, Y.-H. Ra, and C.-R. Lee (2010) *J. Mater. Res.* **25** 1778-1783.

[3] S.-H. Yun, Y.-H. Ra, Y.-M. Lee, K.-Y. Song, J.-H. Cha, H.-C. Lim, D.-W. Kim, N.J.S. Kissinger, C.-R. Lee (2010) *J. Cryst. Growth* **312** 2201-2205.

[4] X.M. Cai, F. Ye, S.Y. Jing, D.P. Zhang, P. Fan, E.Q. Xie (2008) *Appl. Surf. Sci.* **255** 2153-2158.

[5] Y.-K. Chang, F.C.-N. Hong (2009) *Mater Lett* **63** 1855-1858.

[6] C. Nie, R. Zhang, Z.-L. Xie, X.-Q. Xiu, B. Liu, D.-Y. Fu, Q.-J. Liu, P. Han, S.-L. Gu, Y. Shi, Y.-D. Zheng (2008) *Chin Phys Lett* **25** 1780.

[7] Y. Sun, Y.-H. Cho, Z. Dai, W. Wang, H. Wang, L. Wang, S. Zhang, H. Yang (2010) *Physica E* **43** 138-141.

[8] N. Takahashi, A. Niwa, T. Nakamura (2004) *J. Phys. Chem. Solids* **65** 1259–1263.

[9] S.-H. Lee, E.-S. Jang, D.-W. Kim, I.-H. Lee, S. Kannappan and C.-R. Lee (2009) *J. Korean Phys. Soc.* **55** 1070.

[10] G. Xu, Z. Li, J. Baca, J. Wu (2010) *Nanoscale Res. Lett.* **5** 7-13.

[11] F. Zhang, Q. Wu, Y. Zhang, J. Zhu, N. Liu, J. Yang, X. Wang, Z. Hu (2012) *Appl. Surf. Sci.* **258** 9701-9705.

[12] O. Briot, S. Ruffenach, M. Moret, B. Gil, C. Giesen, M. Heuken, S. Rushworth, T. Leese, M. Succi (2009) *J. Cryst. Growth* **311** 2761-2766.

[13] H.J. Park, O. Kryliouk, T. Anderson, D. Khokhlov, T. Burbaev (2007) *Physica E* **37** 142-147.

[14] I. Jung, S. Lee, D. Shin, H. Park, M.Y. Ju and C. Kim (2012) *J. Appl. Cryst.* **45** 503-506.

[15] O. Kryliouk, H.J. Park, Y.S. Won, T. Anderson, A. Davydov, I. Levin, J.H. Kim and J.A. Freitas Jr. (2007) *Nanotechnology* **18** 135606.

[16] A.P. Vajpeyi, A.O. Ajagunna, G. Tsiakatouras, A. Adikimenakis, E. Iliopoulos, K. Tsagaraki, M. Androulidaki, A. Georgakilas (2009) *Microelectron. Eng.* **86** 812-815.

[17] A.O. Ajagunna, A. Adikimenakis, E. Iliopoulos, K. Tsagaraki, M. Androulidaki, A. Georgakilas (2009) *J. Cryst. Growth* **311** 2058-2062.

[18] Z. Mi, H.P.T. Nguyen, K. Cui, X. Han, S. Zhang, and Y.-L. Chang (2010) *Proc. of SPIE* 78477847002-1.

[19] C.H. Liang, L.C. Chen, J.S. Hwang, K.H. Chen, Y.T. Hung, and Y.F. Chen (2002) *Appl. Phys. Lett.* **81** 22.

[20] P.T. Terziyska, K.S.A. Butcher, D. Gogova, D. Alexandrov, P. Binsted, G. Wu (2013) *Mater. Lett.* **106** 155-7.

[21] P.T. Terziyska, K.S.A. Butcher, P. Rafailov and D. Alexandrov *Appl Surf Sci* (2015) **353** 103-105.

[22] K.S.A. Butcher, US Pattent Application: *Migration Enhanced Chemical Vapour Deposition*, US 2010/0210067.

[23] K.S.A. Butcher, B.W. Kemp, I.B. Hristov, P. Terziyska, P.W. Binsted and D. Alexandrov *Jpn. J. Appl. Phys* (2012) **51** 01AF02-1-01AF02-5.

[24] K.S.A. Butcher, D. Alexandrov, P. Terziyska, V. Georgiev, D. Georgieva, and P.W. Binsted *Phys Status Solidi A* (2012) **209** 41-44.

[25] S.N. Mohammad *J Chem Phys* (2006) **125** 094705-21.

[26] W. Kim, M. Yeadon, A.E. Botchkarev, S.N. Mohammad, J.M. Gibson, and H. Morkoç (1997) *J. Vac. Sci. Technol. B* **15** 921-7.

[27] M. Kuball, J.W. Pomeroy, M. Wintrebert-Fouquet, K.S.A. Butcher, H. Luc, W.J. Schaff (2004) *J. Cryst. Growth* **269** 59-65.

[28] M. He, A. Motayed, and S.N. Mohammad (2007) *J. Chem. Phys.* **126** 064704-1-5.

[29] M. He and S.N. Mohammad (2007) *J. Vac. Sci. Technol. B* **25** 940-4.

[30] C.J. Novotny and P.K.L. Yu (2005) *Appl. Phys. Lett.* **87** 203111-3.

[31] S.H. Yun, Y.H. Ra, Y.M. Lee, K.Y. Song, J.H. Cha, H.C. Lim et al. (2010) *J. Cryst. Growth* **312** 2201-5.